

# A Low-Noise Self-Oscillating Mixer Using a Balanced VCO Load

Stanley S. K. Ho, *Member, IEEE*, and Carlos E. Saavedra, *Senior Member, IEEE*

**Abstract**—A low-noise self-oscillating mixer (SOM) operating from 7.8 to 8.8 GHz is described in this paper. Three different components, the oscillator, the mixer core, and the LNA transconductor stage are assembled in a stacked configuration with full dc current-reuse from the VCO to the mixer to the LNA. The LC-tank oscillator also functions as a double-balanced IF load to the low-noise mixer core. A theoretical expression is given for the conversion gain of the SOM taking into account the time-varying nature of the IF load impedance. Measurements show that the SOM has a minimum DSB noise figure of 4.39 dB and a conversion gain of 11.6 dB. Its input  $P_{1\text{ dB}}$  is  $-13.6$  dBm and its output  $P_{1\text{ dB}}$  is  $-2.97$  dBm, while its IIP3 and OIP3 are  $-8.3$  dBm and  $+3.3$  dBm respectively. The chip consumes 12 mW of dc power and it occupies an area of  $0.47\text{ mm}^2$  without pads.

**Index Terms**—Low-noise circuits, mixers, oscillators, self-oscillating mixers, RFICs.

## I. INTRODUCTION

**MIXERS** AND their local oscillators are often designed in a modular fashion meaning that, to a large extent, they are designed as isolated blocks that are eventually interconnected together. However, if the mixer and its local oscillator are viewed as a unified circuit, new and interesting design concepts emerge. The resulting circuits are usually called self-oscillating mixers, or SOMs for short.

A number of different SOM topologies have been demonstrated to date [1]–[9]. In the case of RFIC-based SOMs, the switching core of the Gilbert cell has been used quite frequently because it is a double-balanced structure and it naturally lends itself for integration with differential LC-tank oscillators. In addition, the LC oscillator can be stacked either above [1] or below [2] the switching core depending on particular design needs and considerations. In some SOMs a harmonic frequency of the local oscillator is used in the mixing operation instead of the fundamental signal to enable the SOM to work at higher frequencies [6], [7]. Recently, a SOM capable of operating in two distinct bands, C-band and X-band, was demonstrated by using the oscillator's fundamental tone and its second harmonic in the mixing process [8].

In this paper, a self-oscillating mixer circuit is proposed in which a voltage-controlled oscillator (VCO) structure is stacked

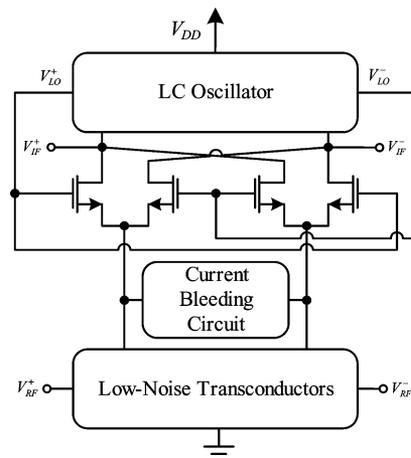


Fig. 1. Block diagram of the proposed VCO-loaded SOM.

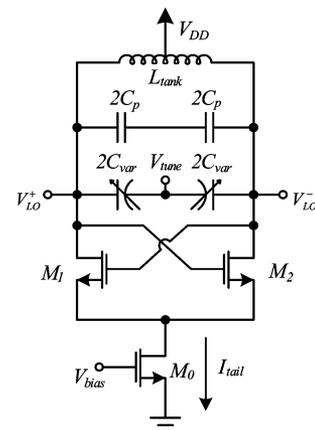


Fig. 2. LC-tank oscillator.

on top of the switching transistors of a Gilbert-type mixing circuit. Thus, in addition to providing the LO signal, the VCO also serves as the IF load to the mixer. Since the VCO is located at the IF section of the mixer, this configuration facilitates the use of a low-noise amplifier (LNA) transconductor stage at the RF input section of the mixer and, as a result, the SOM can achieve a minimum double-sideband (DSB) noise figure of 4.39 dB. Since the VCO, the mixer, and the LNA are all stacked above one another, this topology enables dc current-reuse, thereby simplifying the dc bias circuitry and leading to a reasonably low power consumption of 12 mW. The chip was fabricated using a standard  $0.13\text{-}\mu\text{m}$  CMOS process and it measures  $0.47\text{ mm}^2$  excluding bond pads.

## II. CIRCUIT DESCRIPTION

The block diagram of the proposed VCO-loaded SOM is shown in Fig. 1. The VCO used in this design is derived from the well-known LC-tank oscillator circuit shown in Fig. 2. In

Manuscript July 11, 2010; revised November 12, 2010. Date of publication February 14, 2011; date of current version July 27, 2011. This work was supported in part by a grant from the Natural Sciences and Engineering Research Council of Canada (NSERC). This paper was recommended by Associate Editor A. Neviani.

The authors are with the Department of Electrical and Computer Engineering, Queen's University, Kingston, ON K7L 3N6, Canada (E-mail: saavedra@queensu.ca).

Digital Object Identifier 10.1109/TCSI.2011.2106050

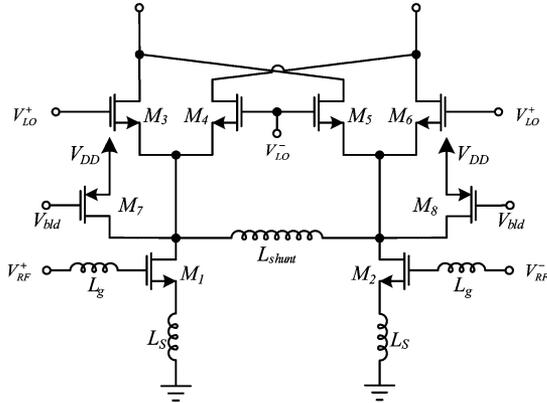


Fig. 3. Low-noise mixer core for the SOM.

this type of oscillator, the varactors used in the LC tank can contribute to the oscillator phase noise through AM-PM conversion due to amplitude noise in  $V_{\text{tune}}$  [10]. Another source of phase noise is the tail transistor because thermal and flicker noise from the tail transistor gets translated into phase noise [11]. Furthermore, since the oscillator is above the mixer core, any noise from the mixer is turned into phase noise. The phase noise of an LC-tank oscillator can be reduced by minimizing the width of the cross-coupled transistors and simultaneously biasing them with a high overdrive voltage while maintaining a  $g_m$  that is large enough for oscillation [12]. Through careful design of the mixer core, the phase noise of the LC-tank VCO used in this work can be reduced, as will be described later in this section.

The LNA transconductors plus mixer core used here is similar to that of [13] but has been modified to suit this SOM and the new circuit schematic is shown in Fig. 3. The mixer core is formed by the following blocks: the low-noise transconductors, a current-bleeding circuit, and the switching pairs. Transistors  $M_1$  and  $M_2$  and inductors  $L_g$  and  $L_s$  form the LNA transconductors, and it was designed using the simultaneous noise and impedance match (SNIM) technique [14]. This design method yields good input matching and achieves minimum noise figure at the same time. As explained in [15], an optimum transistor finger width and gate bias voltage are needed to obtain a minimum noise figure for the LNA.

The switching pairs are formed by transistors  $M_3$ – $M_6$  and the current-bleeding circuit is comprised of transistors  $M_7$  and  $M_8$ . The current-bleeding circuit [16] plays a key role in the operation of the SOM. First, it provides the necessary current to the LNA transconductors and the switching pairs can therefore be biased with a low overdrive voltage, which reduces the LO power needed for switching and makes the switching more ideal.

Second, it reduces the current through the oscillator. Since the dc current through the oscillator is completely reused by the mixer, the current through the switching pairs determines the LO voltage swing. Without the bleeding circuit, all of the current required by the LNA transconductors would flow through the oscillator, causing a very large LO signal not suitable for this design. As explained in the VCO loading section, a large dc current through the cross-coupled pairs will significantly reduce

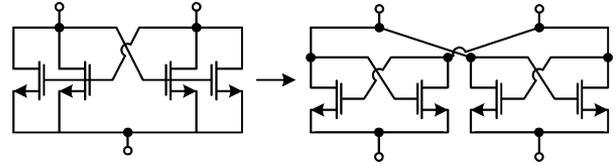


Fig. 4. New VCO cross-coupled configuration to act as mixer load.

the conversion gain. The bleeding circuit is therefore required to ensure the proper operation of the SOM.

Third, it reduces mixer flicker noise. Although the flicker noise of a mixer might seem less important when the IF is at 300 MHz, this is not the case with this particular SOM. Since the mixer current feeds into the LC-tank VCO, the mixer essentially plays the role of the tail transistor of the oscillator. Therefore, flicker noise and thermal noise from the mixer get translated into phase noise. As the flicker noise and thermal noise increase, the phase noise will deteriorate accordingly. The transconductors in the Gilbert-cell mixer can add a noticeable amount of thermal noise [17] and therefore the mixer's noise can be further reduced by using low-noise transconductors, which is the approach taken in this SOM design.

The flicker noise of the switching pairs appears directly at the output without frequency translation, which is caused by the direct and indirect mechanism and is explained in detail in [18]. To minimize the effect of the direct mechanism, the biasing current through the switching pairs should be reduced. Thus, the current-bleeding circuit is used here to lower the dc current flow. The indirect flicker noise mechanism is caused by the tail-capacitance of the switching pairs. By resonating out the capacitance with a parallel inductor,  $L_{\text{shunt}}$ , the indirect flicker noise is reduced and the conversion gain increases.

The bleeding circuit does add some noise to the circuit. Since the noise currents from the bleeding transistors are uncorrelated, each noise current feeds into different switching pairs and their noise contribution appears directly at the output, unlike common-mode noise. To minimize the noise contribution of the bleeding circuit, the PMOS pair is biased at the optimum source-gate voltage for minimum noise.

The most suitable way to connect the oscillator to the mixer is through the source terminal of the cross-coupled pair, but this is a single-ended port while the mixer output is fully differential. Thus, the oscillator circuit in Fig. 2 needs to be modified before it can be stacked on top of the mixer core. Our approach was to reconfigure the cross-coupled transistor pair structure. Noting that a single transistor can be realized by connecting two transistors in parallel, likewise the cross-coupled transistor pair can be realized with four transistors as shown on the left of Fig. 4, where the transistor size is half of the original. This configuration is also the same as connecting two cross-coupled pairs in parallel. The source node of the two cross-coupled pairs can be separated as shown on the right of Fig. 4 because there is no current flowing from one cross-coupled pair into the other through the source node. This new configuration can now be connected to the mixer core and act as a fully balanced load. The dc current through each branch is half of the original value and the size of the transistors is also half of that of the original. The effective

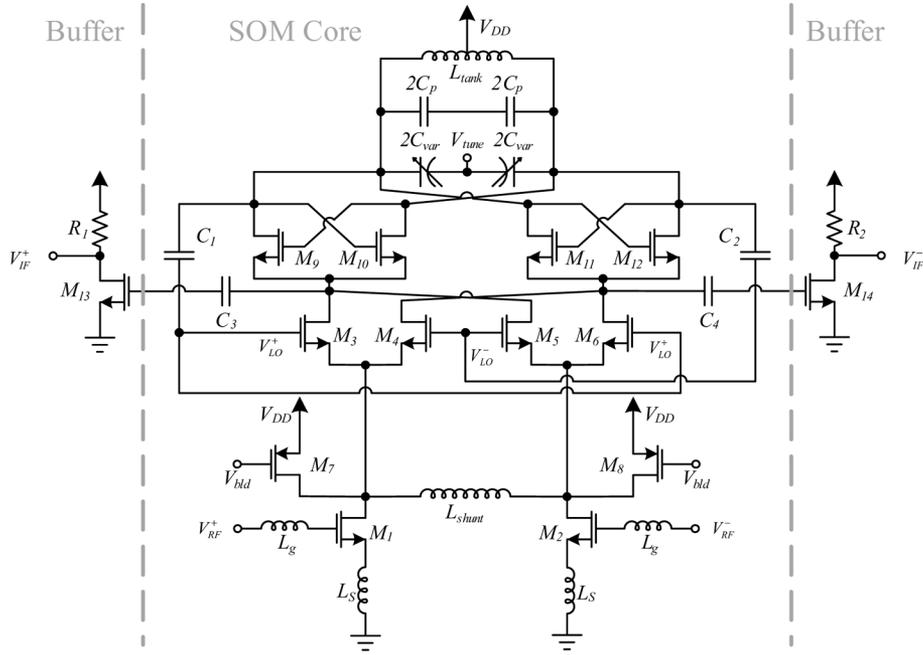


Fig. 5. The complete VCO-loaded SOM circuit schematic.

$g_m$ , dc current, and device size of the oscillator are therefore unchanged compared to the oscillator in Fig. 2.

When the mixer and the modified VCO are merged, the result is the circuit in Fig. 5. The output voltage of the LC tank is fed to the switching pair through two on-chip capacitors in series that act as a dc block. Note that the LNA, mixer and VCO are three different blocks with different functions yet they share the same dc current.

Observing that the capacitances of the switching pairs directly load the LC tank, the oscillating frequency can be expressed as

$$\omega_o = \frac{1}{\sqrt{L_{tank}(C_p + C_{var} + 4C_{gd_o} + C_{gs_o} + C_{gs_s} + C_{gd_s})}} \quad (1)$$

where  $C_{gd_o}$  and  $C_{gs_o}$  are the gate-drain and gate-source capacitance from a cross-coupled transistor and  $C_{gs_s}$  and  $C_{gd_s}$  are the gate-source and gate-drain capacitance of a switching transistor respectively. The output of the SOM is taken differentially at the drains of the switching pair like a normal Gilbert cell and buffers are used so that the SOM is not significantly loaded by the measurement equipment.

Fig. 6 shows the operation of the SOM when  $V_{LO}^+$  is high. The components and nets that are coloured in grey represent the part of the circuit has been turned off and the dotted lines show the RF current flows. When the SOM is in steady-state operation a sinusoidal voltage wave is generated across the LC tank. During the time when Node Plus is positive and Node Minus is negative, transistors  $M_3$ ,  $M_6$ ,  $M_{10}$ , and  $M_{12}$  are turned on while  $M_4$ ,  $M_5$ ,  $M_9$ , and  $M_{11}$  are off. The RF current from  $M_1$  goes through  $M_3$  and  $M_{10}$  towards Node Minus. On the other hand, the RF current from  $M_2$  goes through  $M_{12}$  and  $M_6$  away from Node Minus. Node Minus, therefore, acts as a differential ground for the downconverted RF current. Furthermore, at low

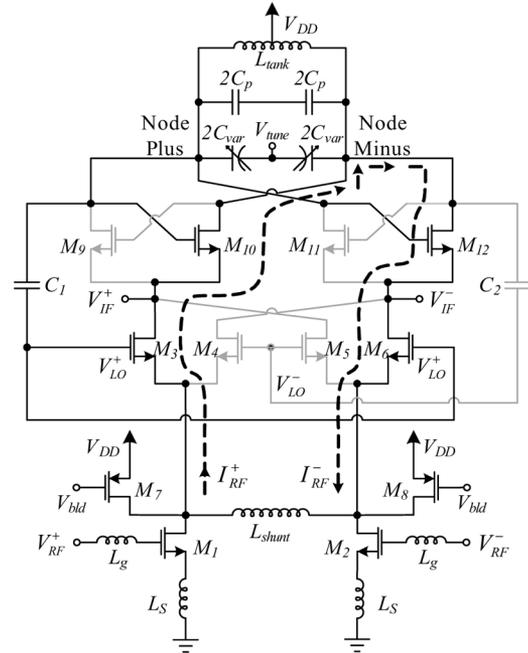


Fig. 6. VCO-loaded SOM during operation when  $V_{LO}^+$  is high.

IF, the symmetrical inductor behaves like a short to  $V_{DD}$ . Thus, the mixer loads are the cross-coupled transistors only.

From Fig. 6, it becomes clear that flicker noise and thermal noise at the fundamental and harmonics of the downconverted signal are all translated into phase-noise. This SOM, however, has a low-noise mixer core that minimizes the thermal noise. Furthermore, care was taken to reduce the mixer flicker-noise that leads to a reduction in phase-noise at low frequency offset.

To derive an expression for the conversion gain of the mixer, the time-varying load impedance of the VCO must first be quantified. Fig. 7 shows the equivalent circuit that was used to derive the input impedance of a cross-coupled pair where  $\Delta V$  is

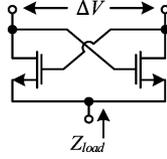


Fig. 7. Circuit used to find  $Z_{load}$  of a cross-coupled pair load.

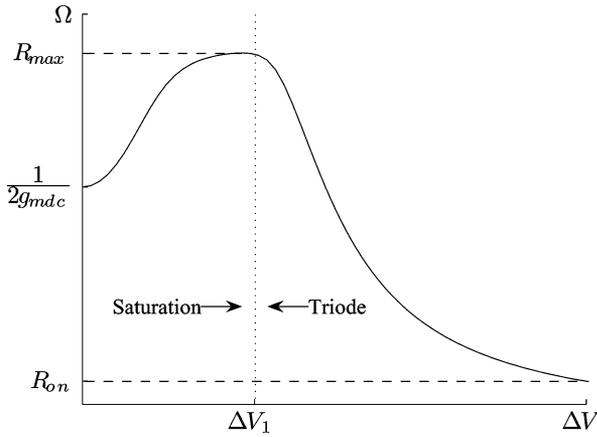


Fig. 8. Simulated load impedance versus LO voltage swing.

the voltage difference between the drains to which the LC tank is connected.  $\Delta V$  can also be expressed as  $V_{gs} - V_{ds}$ . Shown in Fig. 8 is the simulated load impedance of the cross-coupled pair with respect to the LC tank voltage swing. When  $\Delta V$  is 0, both transistors are on and the input impedance is given by  $1/2g_{mdc}$ , where  $g_{mdc}$  is the dc transconductance of a cross-coupled transistor. When  $\Delta V$  increases, one transistor starts to shut off while the other's transconductance,  $g_m$ , is increasing. However, the first transistor turns off at a much faster rate, resulting in a rapid increase in impedance. The  $g_m$  of the other transistor increases at a much slower rate, resulting in a slow decrease in impedance. The combined result is that the input impedance of the cross-coupled pair increases. The loading effect of the off-transistor quickly diminishes and the input impedance of the cross-coupled pair becomes approximately equal to the input impedance of the on-transistor. It increases to its maximum when  $\Delta V$  reaches  $\Delta V_1 = V_{TH}$ , the threshold voltage of the transistor. The on-transistor is still in saturation and  $R_{max}$  is approximately equal to  $1/g_{m_{on}}$ , the input impedance of the on-transistor. Beyond this point, the on-transistor goes into the triode region and its input impedance rapidly drops to its on-resistance,  $R_{on}$ . The optimum LO swing for maximum load is therefore at  $\Delta V_1$ , which is equal to  $V_{TH}$ . Unlike traditional mixers where a large LO swing is desired, a large LO would adversely affect the conversion gain of this SOM.

To simplify the analysis, it is assumed that  $C_{gs}$  and  $C_{gd}$  have negligible effect and the input impedance is equal to the input resistance. Fig. 9 shows a trapezoidal approximation of the variation of the load resistance as a function of time. The load resistance oscillates at twice the LO frequency with a constant dc value. By approximating the plot as a trapezoid, the

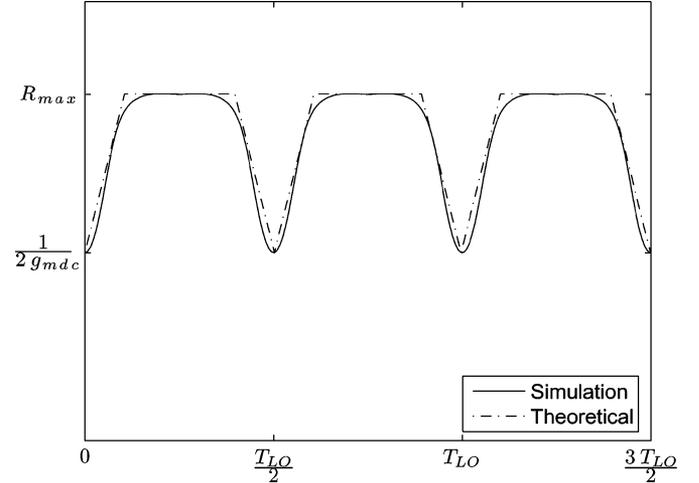


Fig. 9. Simulated  $R_{load}$  versus time.

time-varying load resistance can be expressed by the following Fourier series:

$$R_{load} = R_{max} - \frac{2\tau_r}{T_{LO}} \left( R_{max} - \frac{1}{2g_{mdc}} \right) - \frac{4\tau_r A \sin(\omega_{LO}\tau) \sin(\omega_{LO}\tau_r)}{T_{LO} \omega_{LO}\tau \omega_{LO}\tau_r} \cos(2\omega_{LO}t) + \dots \quad (2)$$

where  $T_{LO}$  is the LO period,  $\tau_r$  is the rise time from the minimum to the maximum,  $\tau = T_{LO}/2 - \tau_r$ , and  $A = R_{max} - 1/2g_{mdc}$ .

Recalling that the effective transconductance of an inductive-degenerated transconductor is

$$g_{m_{eff}} = \frac{g_m \omega (L_s + L_g)}{Z_0} \quad (3)$$

and that the conventional expression for the conversion gain of a Gilbert cell mixer is

$$CG = \frac{2}{\pi} \frac{\sin(\pi f_{LO} t_{sw})}{\pi f_{LO} t_{sw}} g_m R_{load}, \quad (4)$$

where  $t_{sw}$  is the switching time interval during which both switches are on, then the conversion gain equation for the SOM in this paper can be found by substituting (2) and (3) into (4)

$$CG_{SOM} \cong \frac{2}{\pi} \frac{\sin(\pi f_{LO} t_{sw})}{\pi f_{LO} t_{sw}} \frac{g_m \omega (L_s + L_g)}{Z_0} \times \left[ R_{max} - \frac{2\tau_r}{T_{LO}} \left( R_{max} - \frac{1}{2g_{mdc}} \right) \right]. \quad (5)$$

To maximize the conversion gain,  $R_{load}$  should be maximized and since this quantity is related to  $g_{mdc}$ , the lower the transconductance, the larger the gain. This is another reason why a low VCO bias current is desired. Fig. 9 shows the simulated value of  $R_{load}$  versus time and using that graph,  $R_{max}$  is found to be equal to  $110 \Omega$  with  $1/2g_{mdc}$  equal to  $75.7 \Omega$ . Since the LO frequency used in this paper is 8.3 GHz, then  $T_{LO}$  is  $1/f_{LO} = 120$  ps and  $\tau_r$  turns out to be approximately equal to 15.8 ps. From (2), the dc value for  $R_{load}$  is  $101 \Omega$  in this work.

### III. VCO PULLING AND INJECTION-LOCKING

Like most other oscillator circuits, the VCO used in this work is susceptible to the phenomena of frequency pulling and injection-locking [19]–[22]. The VCO and mixing core arrangement in this SOM shares a similar structure to that of injection-locked frequency divider (ILFD) circuits [23], [24]. As a result, when there is an interferer or other signal at the RF input port of the SOM, the IF output currents of the mixer will have components at  $n f_{LO} \pm f_{RF}$ , where  $n$  is an odd integer. When one of those frequency components is in the lock-in range of the VCO, the VCO output will lock to that frequency. In addition, if the frequency tone in question is slightly outside of the lock-in range but not too far away, then the LO signal will get pulled to a different frequency.

In this SOM, one can apply 2 signals at  $2f_{LO}$  to the sources of the cross-coupled pairs to lock the VCO. However, the  $2f_{LO}$  signal must be in-phase with each other. This signal can be generated due to phase and amplitude mismatch at either the RF transconductors or the switching pairs. Another mechanism to generate the signal could be even-order harmonics generated by the transconductors.

For the first mechanism, one particular component that might cause locking/pulling is the upconverted  $f_{LO} + f_{RF}$ . For low IF frequencies, this component is around  $2f_{LO}$ . Due to the differential structure of the mixer and that the cross-coupled pair is split into two, the out-of-phase upconverted  $f_{LO} + f_{RF}$  signals will generate excess phase in the oscillator that cancels each other, resulting in no injection lock under ideal conditions. But because of inevitable mismatch either from layout or process, an in-phase component will appear and possibly lock or pull the VCO. Locking or pulling depends on the amplitude of the injected signal as well as the frequency. For large IF, locking does not happen. The amount of pulling will depend on the amplitude. For very low IF, locking can occur, but it also depends on the signal amplitude. Because of the amplitude dependence, a large input signal and a large mismatch is required. Furthermore, a portion of the  $2f_{LO}$  signal will be attenuated by the tail capacitor at the sources of the cross-coupled pairs, requiring an even larger amplitude. In spite of the similarity between this SOM and ILFDs, this circuit is not as sensitive to locking and pulling as ILFDs. Measurements on the SOM show that when an 8 GHz signal with  $-27$  dBm of power is applied at the RF port, it pulls the free-running VCO signal by just 1 MHz from 8.3 GHz to 8.301 GHz.

For the second mechanism, the even harmonics generated from the transconductors are in-phase at the mixer output. However, since only odd LO harmonics are present, the mixing products are all near the odd harmonics of the LO (eg,  $3f_{LO} - 2f_{RF} \approx f_{LO}$ ), but not even LO harmonics. So it has a lesser impact on VCO locking and pulling.

The effects of the pulling/locking phenomena are generally more prominent at the lower-end of the IF band and there are a couple remedies to mitigate those effects. Since this is a mixer, capacitors to ground can be added at the outputs of the switching pairs, effectively grounding all high frequency currents besides the IF. A better approach is to add a low-pass filter similar to the one used in [25] where it was used to suppress high frequency

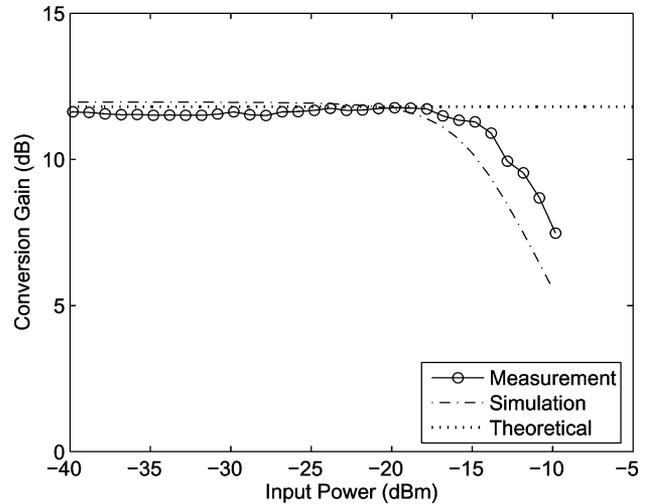


Fig. 10. Measured conversion gain versus input power.

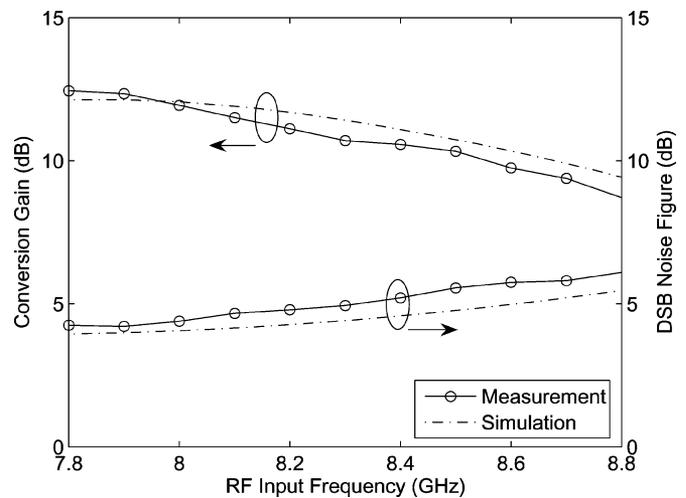


Fig. 11. Measured conversion gain and noise figure versus input frequency with a fixed 300 MHz IF.

noise from the tail transistor. This approach is suitable for this SOM as it a) eliminates any high frequency current that might lock the VCO and b) reduces high frequency noise from the mixer to improve phase noise.

### IV. EXPERIMENTAL RESULTS

A chip was fabricated to demonstrate the performance of the SOM using a standard  $0.13\text{-}\mu\text{m}$  CMOS process. The circuit operates over an RF input range of 7.8 GHz to 8.8 GHz with a tunable LO from 8.1 GHz to over 9 GHz. The IF was kept fixed at 300 MHz in the measurements.

An RF input power versus IF output power measurement was made and from that experiment the conversion gain of the SOM was determined. Fig. 10 shows the conversion gain results as a function of RF input power. We observe that the measured conversion gain was 11.6 dB, which agrees well with both simulation and the theoretical calculation using (5). The conversion gain was also measured as a function of frequency and the results are shown in Fig. 11. The measurements in Fig. 11 were made by sweeping the RF and LO signals together in order to maintain a constant IF output frequency.

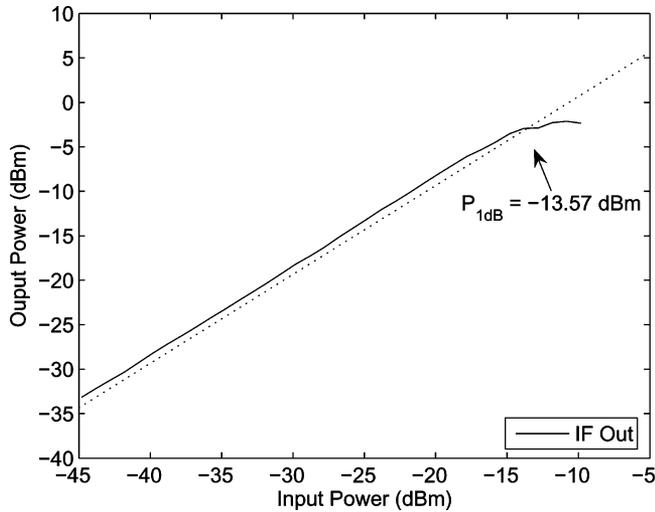


Fig. 12. Measured IF output power with different input power levels.

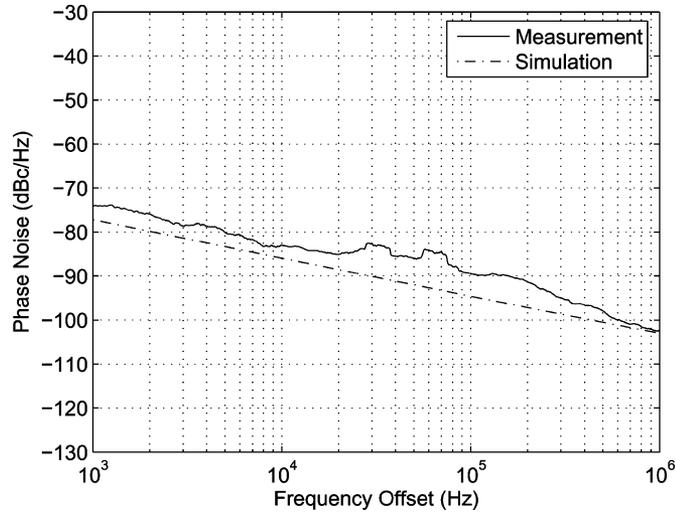


Fig. 13. Measured phase noise of the oscillator signal.

Fig. 12 shows the measured output power versus input power. The measured input  $P_{1\text{ dB}}$  was  $-13.57\text{ dBm}$  and the output  $P_{1\text{ dB}}$  was  $-2.97\text{ dBm}$ .

In SOMs the oscillator subcircuit is completely integrated with the mixing subcircuit and therefore it is common practice to not include output pads for the oscillator signal. Therefore, to measure the phase-noise (PN) of the oscillator subcircuit in this work, an indirect approach was taken, which was to measure the PN of the LO leakage signal at the IF output port. A plot of the measured and simulated PN of the oscillator is shown in Fig. 13.

The double-sideband noise figure (DSB NF) of the complete mixer was measured versus frequency and the results are included in Fig. 11. We observe that the minimum DSB NF for the SOM is  $4.39\text{ dB}$ , which is only  $0.3\text{ dB}$  higher than in simulation.

A two-tone test was carried out to determine the third-order intercept (TOI) point of this SOM. The input RF power was swept and the power level of the IF signals and the intermodulation products were measured. Fig. 14 shows the results of the two-tone test and it is observed that the SOM has an IIP3 of  $-8.3\text{ dBm}$  and an OIP3 of  $+3.3\text{ dBm}$ .

Since the VCO subcircuit is completely integrated into the mixer, no output pads were allocated for the LO signal and therefore the precise LO signal power is unknown. This precluded the

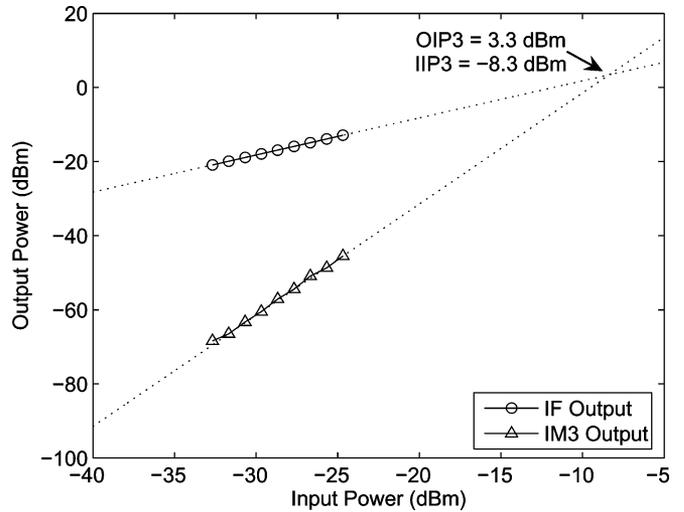


Fig. 14. Measured IF and third order intermodulation product output powers.

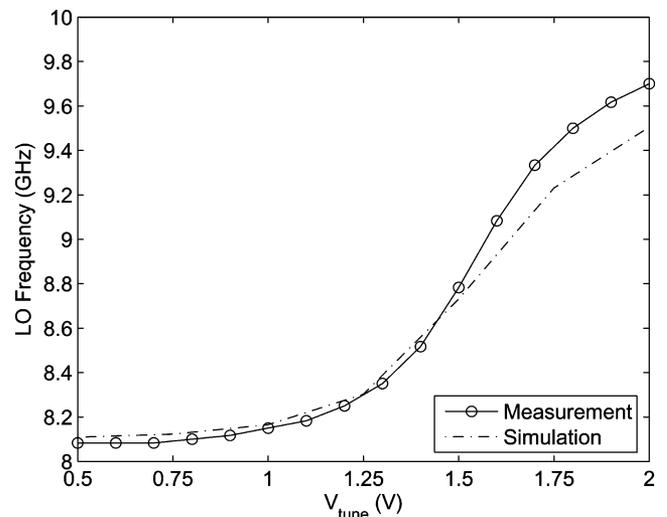


Fig. 15. Measured LO frequency with different values of  $V_{\text{tune}}$ .

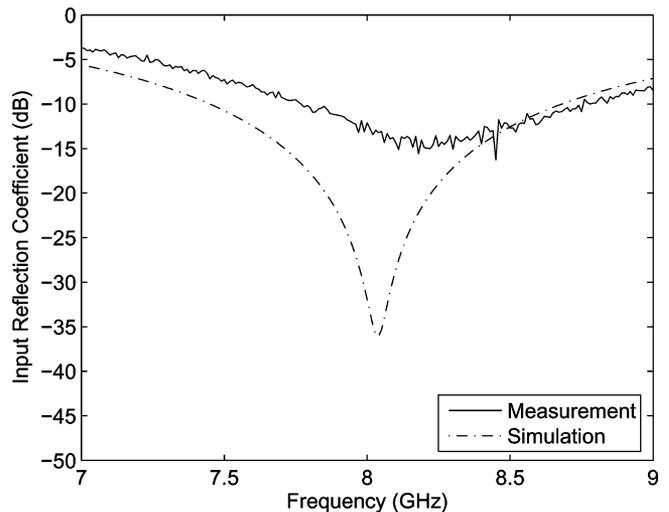


Fig. 16. Measured input reflection coefficient.

measurement of the LO-to-RF isolation. Instead, we measured the LO leakage power at the RF port, which was  $-59.1\text{ dBm}$ . The tuning range of the VCO was determined by measuring the LO leakage signal at the IF port and the results shown in Fig. 15

TABLE I  
PERFORMANCE SUMMARY AND COMPARISON TABLE

	This Work	[1]	[2]	[7]	[8]
Technology	0.13 $\mu\text{m}$ CMOS	0.13 $\mu\text{m}$ CMOS	0.18 $\mu\text{m}$ CMOS	Hybrid	0.13- $\mu\text{m}$ CMOS
RF Freq. (GHz)	7.8 – 8.8	1.57	4.2	10.6 – 11.8	5 – 11.8
Conversion Gain (dB)	11.6	36	10.9	2.5	12 (max)
DSB Noise Figure (dB)	4.39 (min)	4.8	14.5 (SSB)	–	8.7 (min)
Input $P_{1dB}$ (dBm)	–13.6	–31	–	–	–
IIP3 (dBm)	–8.3	–19	–11.8	9.5	5
LO – RF leakage (dBm)	–59	–55	–37	–	–40
Chip size ( $\text{mm}^2$ )	0.47 (core)	1.5 (core)	0.96	N/A	0.53
DC Power (mW)	12 (core)	5.4	3.14	43	68

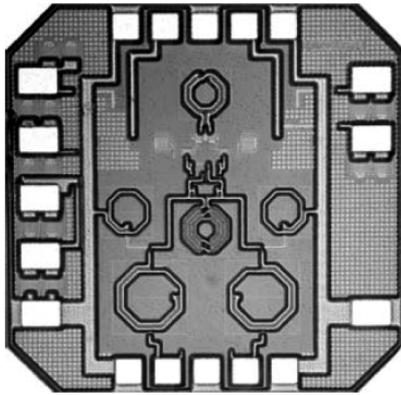


Fig. 17. Microphotograph of the complete low-noise SOM chip.

reveal that the oscillator can be tuned from 8.1 GHz to 9.7 GHz as the control voltage varies from 0.5 V to 2 V. The differential RF input reflection coefficient from 7 GHz to 9 GHz was measured using a vector network analyzer and the results are plotted in Fig. 16.

The entire circuit consumes a total current of 21 mA from a 1.5 V supply. Excluding the output buffers, the SOM consumes only 8 mA of current resulting in a power dissipation of 12 mW for the core. Fig. 17 shows the microphotograph of the SOM chip. The chip occupies an area of 1  $\text{mm}^2$  including pads and 0.47  $\text{mm}^2$  without pads. A performance summary and comparison table between this SOM and other published works is shown in Table I.

## V. CONCLUSION

A double balanced VCO-loaded self-oscillating mixer that uses the VCO as the IF load has been experimentally demonstrated. By stacking the RF transconductor stage, the mixing core, and the oscillator on top of each other, the dc currents can be reused and this leads to a moderately low power consumption. An analysis was carried out and an expression was presented for the conversion gain of the SOM taking into account the time-varying nature of the load impedance. There is good agreement between the theoretical predictions and the measured results.

## ACKNOWLEDGMENT

The authors would like to thank CMC Microsystems, Kingston, ON, Canada, for access to IC fabrication services and Ahmed El-Gabaly for his assistance with measurements.

## REFERENCES

- [1] A. Liscidini, A. Mazzanti, R. Tonietto, L. Vandi, P. Andreani, and R. Castello, "Single-stage low-power quadrature RF receiver front-end: The LMV cell," *IEEE J. Solid-State Circuits*, vol. 41, pp. 2832–2841, Dec. 2006.
- [2] T.-P. Wang, C.-C. Chang, R.-C. Liu, M.-D. Tsai, K.-J. Sun, Y.-T. Chang, L.-H. Lu, and H. Wang, "A low-power oscillator mixer in 0.18- $\mu\text{m}$  CMOS technology," *IEEE Trans. Microw. Theory Tech.*, vol. 54, pp. 88–95, Jan. 2006.
- [3] F. Plessas, A. Papalambrou, and G. Kalivas, "A 5-ghz subharmonic injection-locked oscillator and self-oscillating mixer," *IEEE Trans. Circuits Syst. II, Exp. Briefs*, vol. 55, no. 7, pp. 633–637, 2008.
- [4] C. van den Bos, L. Oliveira, J. Fernandes, and C. Verhoeven, "A 5-ghz combined oscillator/mixer," in *Proc. IEEE Int. Symp. Circuits Syst. (ISCAS)*, Island of Kos, Greece, May 2006, pp. 85–88.
- [5] L. B. Oliveira, J. Fernandes, I. Filanovsky, and C. Verhoeven, "A 2.4 ghz CMOS quadrature lc-oscillator/mixer," in *Proc. IEEE Int. Symp. Circuits Syst. (ISCAS)*, Vancouver, BC, Canada, May 2004, vol. 1, pp. 165–168.
- [6] S. Winkler, K. Wu, and A. Stelzer, "Integrated receiver based on a high-order subharmonic self-oscillating mixer," *IEEE Trans. Microw. Theory Tech.*, vol. 55, pp. 1398–1404, Jun. 2007.
- [7] M. Fernandez, S. Ver Hoeye, L. Herran, and F. Las-Heras, "Nonlinear optimization of wide-band harmonic self-oscillating mixers," *IEEE Microw. Wirel. Compon. Lett.*, vol. 18, pp. 347–349, May 2008.
- [8] B. R. Jackson and C. E. Saavedra, "A dual-band self-oscillating mixer for C-band and X-band applications," *IEEE Trans. Microw. Theory Tech.*, vol. 58, pp. 318–323, Feb. 2010.
- [9] M. Bendak, B. Xavier, and P. Chau, "A 1.2 GHz CMOS quadrature self-oscillating mixer," in *Proc. IEEE Int. Symp. Circuits Syst.*, 1999, vol. 5, pp. 434–437.
- [10] N. Fong, J.-O. Plouchart, N. Zamdmer, D. Liu, L. Wagner, C. Plett, and N. Tarr, "A 1-V 3.8–5.7-GHz wide-band VCO with differentially tuned accumulation MOS varactors for common-mode noise rejection in CMOS SOI technology," *IEEE Trans. Microw. Theory Tech.*, vol. 51, pp. 1952–1959, Aug. 2003.
- [11] A. Hajimiri and T. Lee, "Design issues in CMOS differential LC oscillators," *IEEE J. Solid-State Circuits*, vol. 34, pp. 717–724, May 1999.
- [12] A. Jerng and C. Sodini, "The impact of device type and sizing on phase noise mechanisms," *IEEE J. Solid-State Circuits*, vol. 40, pp. 360–369, Feb. 2005.
- [13] H. Sjoland, A. Karimi-Sanjaani, and A. Abidi, "A merged CMOS LNA and mixer for a WCDMA receiver," *IEEE J. Solid-State Circuits*, vol. 38, pp. 1045–1050, Jun. 2003.
- [14] T.-K. Nguyen, C.-H. Kim, G.-J. Ihm, M.-S. Yang, and S.-G. Lee, "CMOS low-noise amplifier design optimization techniques," *IEEE Trans. Microw. Theory Tech.*, vol. 52, pp. 1433–1442, May 2004.

- [15] E. Morifuji, H. Momose, T. Ohguro, T. Yoshitomi, H. Kimijima, F. Matsuoka, M. Kinugawa, Y. Katsumata, and H. Iwai, "Future perspective and scaling down roadmap for RF CMOS," in *Proc. Symp. VLSI Technol.*, 1999, pp. 163–164.
- [16] J. Park, C.-H. Lee, B.-S. Kim, and J. Laskar, "Design and analysis of low flicker-noise CMOS mixers for direct-conversion receivers," *IEEE Trans. Microw. Theory Tech.*, vol. 54, pp. 4372–4380, Dec. 2006.
- [17] M. Terrovitis and R. Meyer, "Noise in current-commutating CMOS mixers," *IEEE J. Solid-State Circuits*, vol. 34, pp. 772–783, Jun. 1999.
- [18] H. Darabi and A. Abidi, "Noise in RF-CMOS mixers: A simple physical model," *IEEE J. Solid-State Circuits*, vol. 35, pp. 15–25, Jan. 2000.
- [19] B. Razavi, "A study of injection pulling and locking in oscillators," *IEEE J. Solid-State Circuits*, vol. 39, pp. 1415–1424, Sep. 2004.
- [20] S. Daneshgar, O. De Feo, and M. Kennedy, "Observations concerning the locking range in a complementary differential LC injection-locked frequency divider—Part I: Qualitative analysis," *IEEE Trans. Circuits Syst. I, Reg. Papers*, vol. 57, no. 1, pp. 179–188, 2010.
- [21] G. Gangasani and P. Kinget, "Time-domain model for injection locking in nonharmonic oscillators," *IEEE Trans. Circuits Syst. I, Reg. Papers*, vol. 55, no. 6, pp. 1648–1658, 2008.
- [22] P. Maffezzoni, "Analysis of oscillator injection locking through phase-domain impulse-response," *IEEE Trans. Circuits Syst. I, Reg. Papers*, vol. 55, no. 5, pp. 1297–1305, 2008.
- [23] H. Rategh and T. Lee, "Superharmonic injection-locked frequency dividers," *IEEE J. Solid-State Circuits*, vol. 34, pp. 813–821, Jun. 1999.
- [24] S. Verma, H. Rategh, and T. Lee, "A unified model for injection-locked frequency dividers," *IEEE J. Solid-State Circuits*, vol. 38, pp. 1015–1027, Jun. 2003.
- [25] P. Andreani and H. Sjolund, "Tail current noise suppression in RF CMOS VCOs," *IEEE J. Solid-State Circuits*, vol. 37, pp. 342–348, Mar. 2002.



**Stanley S. K. Ho** (S'07–M'10) received the B.A.Sc. degree in electrical engineering from University of British Columbia (UBC), Vancouver, Canada, and the M.Sc. (Eng.) degree in electrical engineering from Queen's University, Kingston, ON, Canada.

His research interests are in the field of RF CMOS integrated circuits such as LNAs, mixers, oscillators, frequency multipliers, and filters.



**Carlos E. Saavedra** (S'92–M'98–SM'05) received the B.Sc. degree from the University of Virginia, Charlottesville, and the M.Sc. and Ph.D. degrees from Cornell University, Ithaca, NY, all in electrical engineering.

From 1998 to 2000 he was with Millitech Corporation, South Deerfield, MA. Since 2000 he has been at Queen's University in Kingston, ON, Canada, where he is currently an Associate Professor. He served as Graduate Chair for the Department of Electrical and Computer Engineering from 2007 to 2010. His re-

search activities are in the field of RF integrated circuits for broadband communications as well as radar and automotive applications.

Dr. Saavedra is a registered Professional Engineer (P. Eng.) in the province of Ontario, Canada. He is the Chair of the IEEE MTT-S Technical Coordinating Committee 22: Signal Generation and Frequency Conversion, he is a member of the Technical Program Committee of the IEEE RFIC Symposium, and is a Reviewer for the IEEE TRANSACTIONS ON CIRCUITS AND SYSTEMS—PART I: REGULAR PAPERS, IEEE TRANSACTIONS ON CIRCUITS AND SYSTEMS—PART II: EXPRESS BRIEFS, IEEE TRANSACTIONS ON MICROWAVE THEORY AND TECHNIQUES, IEEE MICROWAVE AND WIRELESS COMPONENT LETTERS, and *Electronics Letters*.